

## Non-isothermal Deblocking Studies of Amine Blocked Isocyanates and their Validation Using Numerical Simulation Calculations

Vennila Srinivasan<sup>1</sup>, Sumalatha Vasam<sup>2</sup>, Sankar Govindarajan<sup>1\*</sup>

<sup>1</sup>Department of Polymer Science, University of Madras, Guindy Campus, Chennai, Tamil Nadu, India, <sup>2</sup>Department of Physics, IIT Madras, Chennai, Tamil Nadu, India

### ABSTRACT

Influences of isocyanate structure, analytical techniques, and heating rate on deblocking reactions were studied. A series of N-Methylaniline blocked isocyanates with different isocyanates were synthesized. Their solid and solution state deblocking reactions were carried out and studied using different analytical techniques as well as different heating rates. The results indicate that isocyanate structure, the effect of heating rate, analytical method, and state of the blocked isocyanate strongly influence the deblocking reaction. Solution state deblocking reaction always occurs at lower temperatures compared to solid-state reactions. Aromatic isocyanate-based blocked isocyanates deblock at lower temperatures compare to aliphatic isocyanate-based blocked isocyanates. The energy of activation ( $E_a$ ) for deblocking reaction was determined using conversion degree values obtained from Thermo-gravimetric analysis and with the help of Friedmann-Reich-Levi and Flynn-Wall-Ozawa equations. Experimentally determined  $E_a$  was validated using numerical simulation calculations.

**Key words:** Blocked isocyanates, Deblocking, Friedmann-Reich-Levi, Flynn-Wall-Ozawa, Non-isothermal kinetics, Simulation.

### 1. INTRODUCTION

Polyurethanes (PU) are widely used in the polymer industry as well as in everyday life. PU with various properties are used in a variety of applications such as apparel [1,2], appliances, automotive [3,4], flooring, furnishings, medical [5,6], marine [7], building and construction [8,9], composite wood [9], electronics [10], and packaging [11]. It can be produced by the reaction of isocyanates and polyols. However, the difficulty is that isocyanates have a high reactivity to polyol, which makes most PU applications difficult. It is necessary to combine both reactants just prior to use, implying that it can only be used as two packages (2K) PU applications systems. However, 2K systems have drawbacks such as expensive mixing equipment costs, exposure to harmful isocyanates and their transportation to the application site, and so on. As a result, a single package (1K) system, i.e., blocked isocyanates, is an alternative to PU systems. The idea of blocked isocyanate has been well explored elsewhere [12,13].

Recently, Choi *et al.* [14] reported that the effect of the structural configurations of imidazole-based blocking agents on the degree of their dissociation from blocked isocyanate cross-linkers and cross-linking behavior of clear coats during the thermal curing process and then also investigated the correlation between the structures of blocking agents and their deblocking temperature using density functional theory (DFT) simulation. Olejinik *et al.* [15] presented a thorough investigation of different chemical processes that occur during cross-linking of complex commercial PU systems using non-isothermal Differential scanning calorimetry (DSC) and their activation energy was determined by Kissinger-Akahira-Sunose (KAS) and Ozawa-Flynn-Wall (OFW). Dominika *et al.* [16] developed the renewable sources-based blocked polyisocyanates with lower deblocking temperature as a crosslinkers for hydrophobic thermosetting PU powder clear coatings dedicated for medium density fibreboards or wood.

To produce a PU heat-cured system, the blocked isocyanates and polyol resin were heated to the deblocking temperature of the specific blocked isocyanate. Therefore, knowing the deblocking temperature is critical for ideal 1K systems. As a consequence, several studies have been conducted to evaluate the correlation between the structures of blocking agents and their deblocking temperature [17-21]. However, limited study has been conducted to determine how other variables such as isocyanate structure, analytical methods employed, and heating rate influence on deblocking temperature [22,23]. The impact of heating rate, in particular, on deblocking temperature, is critical. Unfortunately, no systematic study has been done to our knowledge to investigate the influence of different deblocking analytical techniques and their heating rate on deblocking temperature. Using the Friedmann-Reich-Levi (FRL) and Flynn-Wall-Ozawa (FWO) equations, one attempt was made to analyze the influence of heating rate on deblocking temperature [22]. They did, however, employ experimental data and curve fitting, and there is no confirmation of their experimental data, which leads to an ambiguous understanding of the link between heating rate and deblocking temperature. Verification of the experimental deblocking process, on the other hand, is critical since this reaction is truly quite complicated.

With this background, we synthesized several N-Methylaniline (NMA) blocked isocyanates and determined deblocking temperatures using

### \*Corresponding author:

E-mail: gsankarphd@gmail.com

ISSN NO: 2320-0898 (p); 2320-0928 (e)

DOI: 10.22607/IJACS.2021.903015

Received: 25<sup>th</sup> July 2021;

Revised: 17<sup>th</sup> August 2021;

Accepted: 19<sup>th</sup> August 2021

different analytical techniques, such as Thermo-gravimetric analysis (TGA), DSC, and CO<sub>2</sub> evolution methods with different heating rates to establish a relationship between heating rate and deblocking temperature and validated experimental results with theoretical numerical simulation calculations using MATLAB software.

## 2. EXPERIMENTAL

### 2.1. Materials

NMA (Lancaster Synthesis Ltd, Mumbai, India), 4,4'-methylene bis (phenyl isocyanate) (MDI) (Lancaster Synthesis Ltd, Mumbai, India), toluene, 2,4-diisocyanate (TDI) (Aldrich, Chennai, India), isophorone diisocyanate (IPDI) (Aldrich, Chennai, India), hexamethylene diisocyanate (HDI) (Aldrich, Chennai, India), poly (tetrahydrofuran) (Terathane, Mn=2000) (Aldrich, Chennai, India), DBTDL (Aldrich, Chennai, India) were used as received. Barium hydroxide (Sisco Research Laboratory, Chennai, India), Hexane (Sisco Research Laboratory, Chennai, India), toluene (Sisco Research Laboratory, Chennai, India), CCl<sub>4</sub> (Sisco Research Laboratory, Chennai, India), DMF (Sisco Research Laboratory, Chennai, India) were used as received after distillation.

### 2.2. Measurements

Fourier-transform infrared (FTIR) spectra of compounds were recorded on Thermo-Mattson Satellite model FTIR spectrophotometer (Thermo Scientific, Chennai, India) by KBr pellet methods. TGA was carried out in a NETZSCH-STA 409 PC thermal analyzer (Netzsch Technologies India Pvt Ltd, Chennai, India) from 30°C to 700°C at a heating rate of 20°C/min under a nitrogen atmosphere with a gas flow rate of 90 mL/min. DSC was performed with NETZSCH-DSC 204 PC instrument (Netzsch Technologies India Pvt Ltd, Chennai, India). The sample was heated from -100°C to 250°C, cooled rapidly, and reheated under nitrogen atmosphere. The heating rate was 10°C/min. Shalom oil bath (Shalom Instruments, Bangalore, India) with digital temperature controller was used for CO<sub>2</sub> evolution experiments.

### 2.3. Preparation of Blocked Diisocyanates

#### 2.3.1. Synthesis of NMA blocked diisocyanate adducts

In a typical experiment, 5 g of NMA and 0.1 g of DBTDL were dissolved in 50 mL of dry toluene and this solution was taken in a 250 mL three-necked round-bottomed flask fitted with a magnetic stirrer and a nitrogen inlet. An equimolar amount of diisocyanates in 50 mL of dry toluene was taken in an addition funnel and fitted with the reaction flask. The isocyanate solution was added dropwise to the round-bottomed flask over 30 min with stirring under nitrogen atmosphere. The reaction was carried out at 50°C for overnight. The blocked isocyanate adduct was precipitated by hexane, filtered, and dried in vacuum desiccators.

#### 2.3.2. Synthesis of NMA blocked polyisocyanates

Two equivalents of Diisocyanate were taken in a three-necked round bottom flask fitted with a mechanical stirrer and a nitrogen inlet. One equivalent of polyol (Terathane 2000) was added dropwise to the flask using an addition funnel with stirring. The reaction temperature was initially held at 50°C for 2 h, then raised to 70°C and the reaction was continued for three more hours. The reaction mixture was then allowed to cool to 40°C. Finally, an equimolar quantity of N-methyl aniline was added to the reaction mixture, and the reaction was allowed to run overnight at 40°C.

### 2.4. CO<sub>2</sub> Evolution Method

The lowest de-blocking temperatures of the blocked diisocyanates in solution were determined using the CO<sub>2</sub> evolution technique.

In a typical experiment, 0.5 g of blocked isocyanate was added to a 100 mL two-neck round-bottom flask with 20 mL of DMF and 5 mL of water. One neck was attached to the nitrogen gas inlet, which feeds CO<sub>2</sub>-free dry nitrogen gas, and the other neck was linked to the purging tube, which was submerged in a saturated solution of barium hydroxide. Initially, the reaction temperature was controlled at 30°C by stirring with a magnetic stirrer. In a silicone oil bath, the flask was heated at 1°C/min, 2°C/min, or 3°C/min. As de-blocking takes place, the regenerated -NCO combines with the available water, releasing carbon dioxide. This carbon dioxide then interacts with the saturated barium hydroxide solution, resulting in turbidity owing to the creation of insoluble barium carbonate. The lowest de-blocking temperature was determined to be the temperature at which noticeable turbidity develops.

### 2.5. Numerical Simulation Calculations

For numerical simulation computations, Matlab software was employed. TGA of BI-6 performed three heating rates, namely 10°C, 20°C, and 30°C per min ( $\beta$ ) to calculate the temperature at which various degrees of conversions ( $\alpha$ ) occur. The  $\alpha$  values are estimated only for the initial weight loss, which is due to the deblocking reaction. The Ea values for the deblocking reaction for each  $\alpha$  were calculated by plugging  $\beta$  and temperature values into the FRL and FWO equations. To get numerical simulation calculations, experimentally determined Ea and A values are fed into the FRL and FWO equations.

## 3. RESULTS AND DISCUSSION

### 3.1. Synthesis of Blocked Isocyanates

N-Methyl aniline blocked isocyanate adducts and polyisocyanates were synthesized, and the blocking reaction was confirmed by FTIR spectroscopy. The FTIR spectra of all the blocked isocyanates are recorded and found to be almost similar. The disappearance of the peak at 2250 cm<sup>-1</sup> (Figure 1), which corresponds to -N=C=O (str), indicates that the reaction between isocyanate and a blocked agent has been completed. The appearance of two additional peaks at 3300 cm<sup>-1</sup> and 1700 cm<sup>-1</sup>, corresponding to -NH (str) and -C=O (str), demonstrates the formation of blocked isocyanates.

### 3.2. Deblocking Studies

TGA [24], DSC [25], and CO<sub>2</sub> [26] evolution techniques were used to estimate the deblocking temperatures of NMA blocked diisocyanates. The estimation of deblocking temperature using hot-stage FTIR spectroscopy was disclosed in our earlier research [18-20].

### 3.3. TGA

Figures 2 and 3 show thermogravimetric graphs of NMA blocked diisocyanate adducts and polyisocyanates, respectively. The heating rate was set to 20°C/min. The temperature at which, 5% weight loss has considered as deblocking temperature. Table 1 shows the deblocking temperature of blocked isocyanates and polyisocyanates. The TDI-based BI adduct exhibits the lowest deblocking temperature of the four blocked isocyanate adducts tested. Because of the electron-withdrawing nature of the aromatic moiety, which drains electron density at the Nitrogen atom present in the blocked isocyanate moiety, aromatic isocyanates deblock at a lower temperature than diisocyanates based on aliphatic ones, making the bond formed during the blocking reaction more labile. Another explanation for TDI's low deblocking temperature is the presence of a methyl group in ortho to the isocyanate molecule. Because of the inductive effect provided by the methyl group present in the benzene ring, the deblocking process is expedited. IPDI has a lower deblocking temperature than HDI in the case of aliphatic isocyanates. This might be due to the IPDI's secondary isocyanate

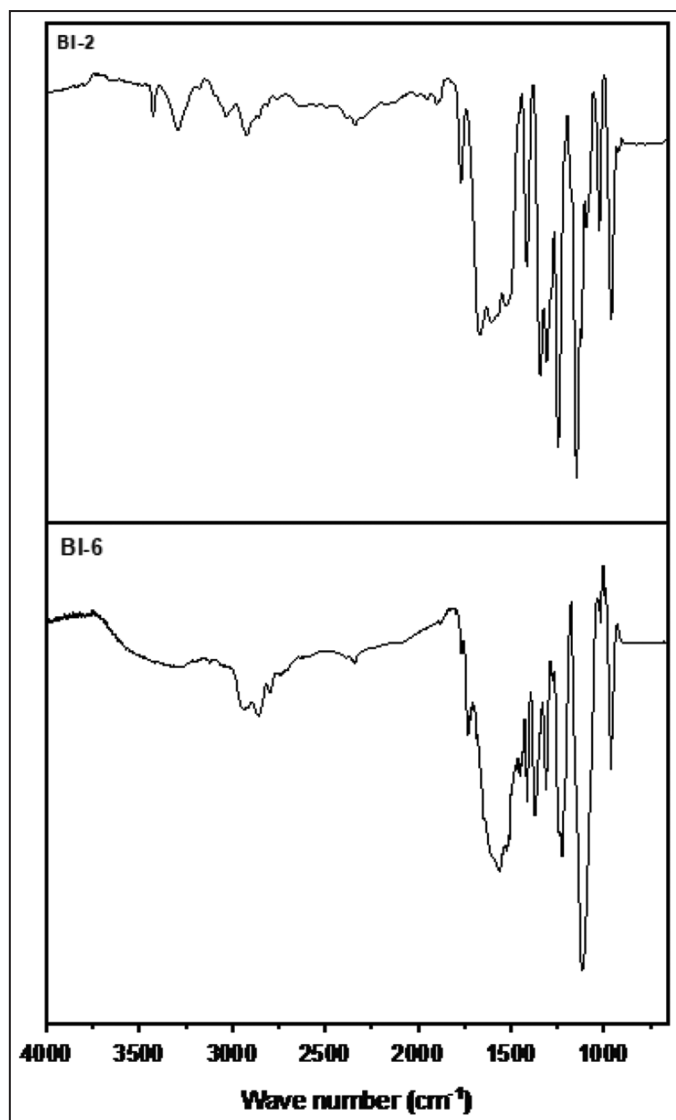


Figure 1: Fourier transform infrared Spectrum of 4,4'-methylenebis(phenylisocyanate) blocked N-methylaniline adduct and polyisocyanate (BI-2 and 6)

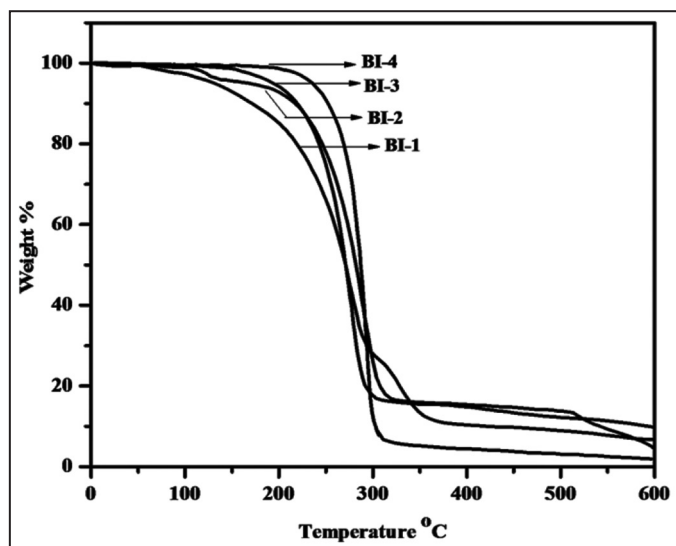


Figure 2: Thermo-gravimetric analysis curves of Blocked isocyanate adducts (BI 1-4)

group. Because of the electron-donating character of Terathane 2000 in the blocked polyisocyanates, it is discovered that blocked polyisocyanate block at a lower rate than corresponding blocked isocyanate adducts. As a result, the bond formed during the blocking reaction is extremely strong and difficult to break.

### 3.4. DSC

Figures 4 and 5 exhibit DSC curves for blocked isocyanate adducts and polyisocyanates, respectively. All of the blocked isocyanate adducts have two endothermic curves. The melting point of blocked isocyanate adducts is shown by the first endothermic curve. All of the adducts have a sharp melting point that is extremely near to the experimentally determined melting point. Because solubility and miscibility of blocked isocyanate with polyol is the key factor in IK PU to build flawless systems, melting point is highly crucial data for blocked isocyanates. The deblocking reaction causes the second endothermic transition. The temperature at the start of the endothermic curve is regarded as the deblocking temperature of the blocked isocyanate adducts (Table 1). The absence of sharp melting points in the blocked polyisocyanates is owing to the presence of oligomeric moieties in the polyisocyanates.

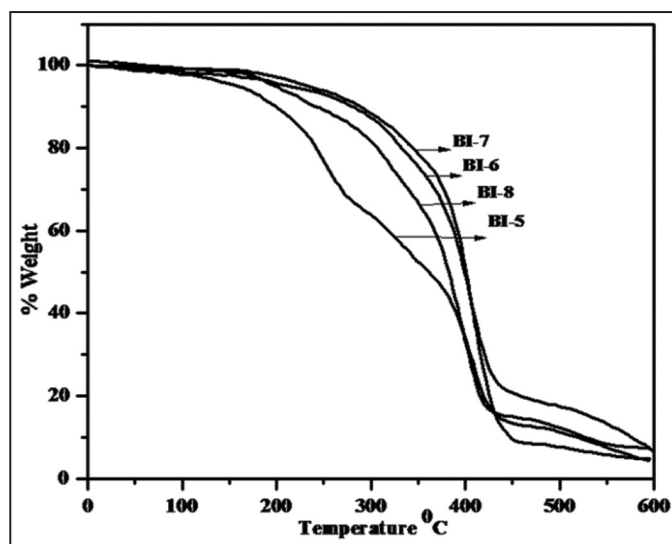


Figure 3: Thermo-gravimetric analysis curves of Blocked polyisocyanate (BI 5-8)

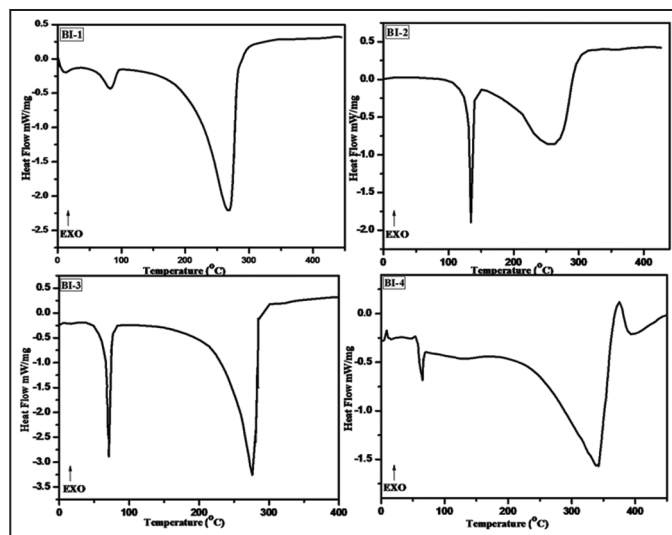


Figure 4: Differential scanning calorimetry graphs of Blocked isocyanate adducts (BI 1-4)

An endothermic curve that begins above 100°C is caused by the deblocking of NMA and polyisocyanates, while a second endothermic curve that begins around 300 °C is caused by the cleavage of the PU link created between diisocyanates and polyol.

### 3.5. CO<sub>2</sub> Evolution Method

The CO<sub>2</sub> evolution technique has the best deblocking temperature when compared to other approaches. Because some applications require blocked isocyanates to be in a solution condition, the deblocking temperature obtained by this approach is significant. Figures 6 and 7 exhibit graphs of deblocking temperature versus heating rate for blocked isocyanate adducts and polyisocyanates, respectively. When compared to all other solid-state technologies, this approach has the lowest deblocking temperature (Table 2). In contrast to prior approaches, the deblocking temperatures of the blocked isocyanate adducts were found to be lower than those of the blocked polyisocyanates. This is due to the possibility of free molecular mobility, which causes more collisions of the blocked isocyanate adducts in solution. The large molecular weight bulky structure of blocked isocyanates based on polyisocyanates, on the other hand, restricts free molecular mobility of the blocked polyisocyanates. When compared to blocked isocyanate adduct, IPDI-based blocked polyisocyanate deblocks at a lower temperature. This is due to the fact that the catalyst used to prepare IPDI-based blocked polyisocyanate (BI-8) is still present in the solution. As a result, the catalytic effect is responsible for the BI-8's low deblocking temperature.

A higher heating rate leads to a higher deblocking temperature. As a result, when compared to other heating rates, 1°C/min provides

**Table 1:** Deblocking temperatures of blocked isocyanates determined by TGA and DSC

| S.No | Sample Code | Blocked Isocyanate | Deblocking Temperature (°C) |     |
|------|-------------|--------------------|-----------------------------|-----|
|      |             |                    | TGA                         | DSC |
| 1    | BI-1        | TDI-NMA            | 138                         | 177 |
| 2    | BI-2        | MDI-NMA            | 205                         | 185 |
| 3    | BI-3        | HDI-NMA            | 242                         | 195 |
| 4    | BI-4        | IPDI-NMA           | 212                         | 168 |
| 5    | BI-5        | TDI-TER-NMA        | 138                         | 118 |
| 6    | BI-6        | MDI-TER-NMA        | 200                         | 124 |
| 7    | BI-7        | HDI-TER-NMA        | 208                         | 142 |
| 8    | BI-8        | IPDI-TER-NMA       | 202                         | 140 |

**Table 2:** Deblocking temperatures of blocked isocyanates determined by CO<sub>2</sub> evolution method

| S.No | Sample Code | Blocked Isocyanate | Deblocking Temperature (°C) |          |          |
|------|-------------|--------------------|-----------------------------|----------|----------|
|      |             |                    | 1 °C/min                    | 2 °C/min | 3 °C/min |
| 1    | BI-1        | TDI-NMA            | 45.5                        | 50.1     | 65.2     |
| 2    | BI-2        | MDI-NMA            | 54.4                        | 57.6     | 63.2     |
| 3    | BI-3        | HDI-NMA            | 53.4                        | 62.4     | 68.9     |
| 4    | BI-4        | IPDI-NMA           | 99.2                        | 129.7    | 138.3    |
| 5    | BI-5        | TDI-TER-NMA        | 58.7                        | 67.3     | 78.2     |
| 6    | BI-6        | MDI-TER-NMA        | 61.3                        | 67.5     | 81.2     |
| 7    | BI-7        | HDI-TER-NMA        | 84.6                        | 98.7     | 102.2    |
| 8    | BI-8        | IPDI-TER-NMA       | 85.7                        | 88.1     | 98.6     |

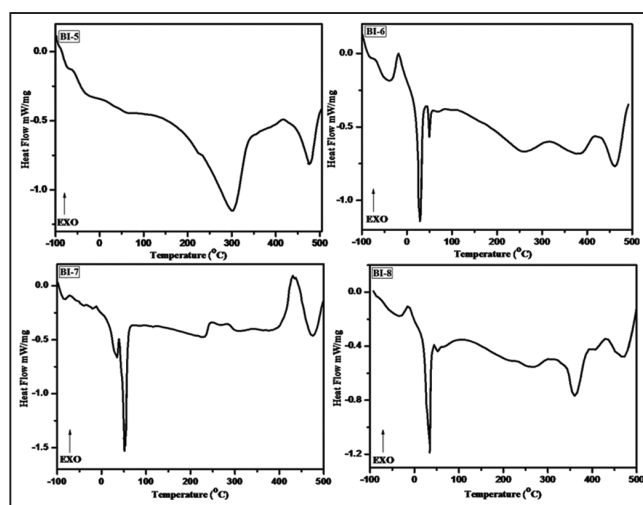


**Figure 5:** Differential scanning calorimetry graphs of Blocked polyisocyanates (BI 5-8)

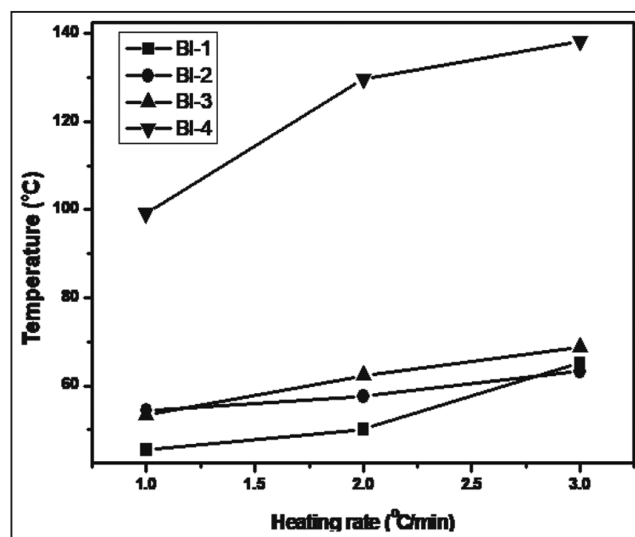


**Figure 6:** Effects of heating rates on deblocking temperatures of BI adducts (BI 1-4)

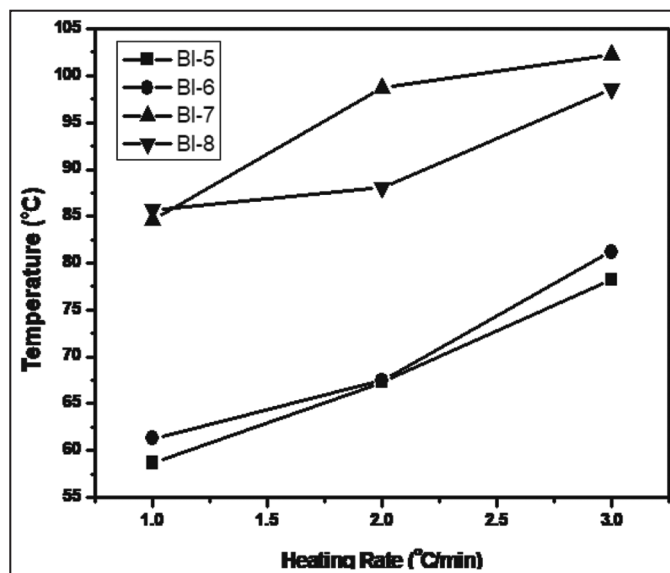


**Figure 7:** Effect of heating rate on deblocking temperatures of blocked polyisocyanates (BI 5-8)



the lowest deblocking temperature. This result is inconsistent with other researchers who study the decomposition reaction of various compounds. [27-29]

### 3.6. Melting Points of Blocked Isocyanates

Melting points of blocked isocyanates are an essential characteristic because efficient curing of blocked isocyanates is dependent on homogeneous mixing of blocked isocyanates with polyols. This is simply accomplished using low melting blocked isocyanates. It was discovered that all of the reported blocked isocyanates are low melting. Melting points determined experimentally are pretty similar compared to DSC melting points (Table 3) (Scheme 1 and 2).

### 3.7. Numerical Calculations

The energy of activation (Ea) for the deblocking reaction of BI-6 was determined using the FRL [30,31] and FWO [32,33] equations. These are obtained from the solid-state non-isothermal reaction equation (eq. 1). The logarithmic form of this equation is known as the FWO equation (eq. 2), and integration of this leads to the FRL equation (eq. 2).

$$\frac{d\alpha}{dT} = \left[ \frac{A}{\beta} \right] e^{\left( -\frac{Ea}{RT} \right)} [f(\alpha)] \quad (1)$$

$$\ln \left[ \beta \left( \frac{d\alpha}{dT} \right) \right] = \ln [A f(\alpha)] - \frac{Ea}{RT} \quad (2)$$

$$\ln[\beta] = \log \left[ \frac{AEa}{R f(\alpha)} \right] - 2.315 - 0.456 \frac{Ea}{RT} \quad (3)$$

Where  $\alpha$  is a degree of conversion,  $\beta$  is a heating rate, A is Arrhenius constant, R is gas constant, Ea is the Ea and T is temperature. The degree of conversion is expressed as follows.

$$\alpha_n = \frac{m_0 - m_n}{m_0 - m_\infty} \quad (4)$$

Where  $m_0$  is the mass of the initial sample,  $m_n$  is the mass of the sample at temperature T and  $m_\infty$  is the final mass.

TGA of BI-6 was performed at three different heating rates ( $\beta$ ) and is shown in Figure 8. Table 4 shows the calculated degrees of conversion for non-isothermal deblocking reactions at various  $\beta$  levels. The

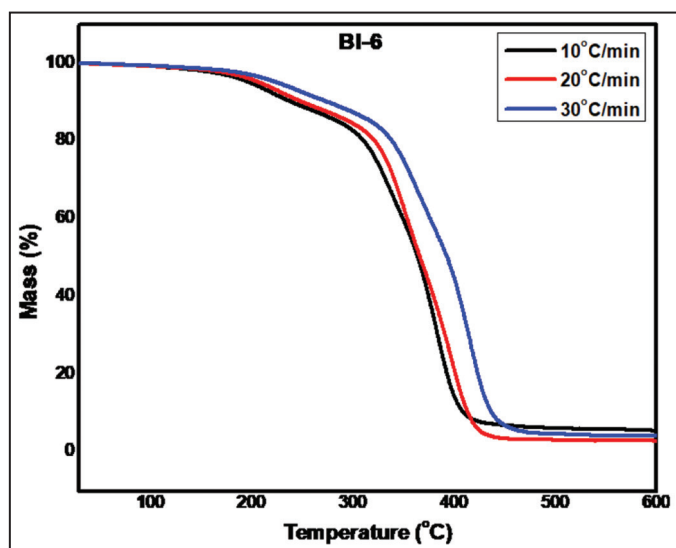


Figure 8: Thermo-gravimetric analysis Graphs of Blocked polyisocyanate 6 at different heating rates

temperature required for various degrees of conversion rises as  $\beta$  values rise.

The Ea and Pre-exponential factor (A) were calculated using the FWO and FRL equations from plots of  $\ln\beta$  versus  $1/T$  and  $\ln(\beta(d\alpha/dT))$  versus  $1/T$ , as illustrated in Figures 9 and 10. In MATLAB, experimentally determined parameters such as Ea, A, and were utilized to create numerical simulations. The results of these simulation computations utilizing this experimental data for both the FWO and FRL equations are depicted in graphs Figures 9b and 10b. Table 5 compared Ea values computed using simulated graphs to the values obtained from experimental findings and graphical representation of correlation curves for degree of conversion ( $\alpha$ ) versus activation energy for both equations are given in Figure 11. For both the FRL and FWO equations,

Table 3: Melting points of blocked isocyanates determined by experimental and DSC

| S.No | Sample Code | Blocked isocyanates | Melting temperature (°C) |              |
|------|-------------|---------------------|--------------------------|--------------|
|      |             |                     | DSC                      | Experimental |
| 1    | BI-1        | TDI-NMA             | 105                      | 95           |
| 2    | BI-2        | MDI-NMA             | 165                      | 165          |
| 3    | BI-3        | HDI-NMA             | 105                      | 106          |
| 4    | BI-4        | IPDI-NMA            | 49                       | Waxy         |
| 5    | BI-5        | TDI-TER-NMA         | No melting               | Waxy         |
| 6    | BI-6        | MDI-TER-NMA         | 19.2 & 37.3              | Waxy         |
| 7    | BI-7        | HDI-TER-NMA         | 23.3 & 39.6              | Waxy         |
| 8    | BI-8        | IPDI-TER-NMA        | 20.4 & 36.4              | Waxy         |

Table 4: Temperatures needed for different degrees of conversion blocked polyisocyanate 6 at different heating rate

| A          | 0.10 | 0.11 | 0.12 | 0.13 | 0.14 | 0.15 | 0.16 | 0.17 | 0.18 | 0.19 | 0.20 |
|------------|------|------|------|------|------|------|------|------|------|------|------|
| $\beta=10$ | 509  | 518  | 527  | 536  | 545  | 553  | 561  | 567  | 572  | 577  | 581  |
| $\beta=20$ | 521  | 531  | 540  | 550  | 559  | 567  | 574  | 580  | 585  | 590  | 593  |
| $\beta=30$ | 546  | 556  | 565  | 573  | 581  | 588  | 594  | 599  | 604  | 607  | 610  |

Table 5: The energy of activation for blocked polyisocyanate 6 was determined from experimental and simulation using FWO and FRL equation

| S.No | $\alpha$ | Ea (kJ/mol)  |            |              |            |
|------|----------|--------------|------------|--------------|------------|
|      |          | FWO Equation |            | FRL Equation |            |
|      |          | Experimental | Simulation | Experimental | Simulation |
| 1    | 0.10     | 141.20       | 140.86     | 182.00       | 241.54     |
| 2    | 0.11     | 143.97       | 143.97     | 185.73       | 247.39     |
| 3    | 0.12     | 148.82       | 148.82     | 192.45       | 256.24     |
| 4    | 0.13     | 160.55       | 160.55     | 208.34       | 274.32     |
| 5    | 0.14     | 170.88       | 170.87     | 222.45       | 290.64     |
| 6    | 0.15     | 181.29       | 181.30     | 236.73       | 306.93     |
| 7    | 0.16     | 196.47       | 196.46     | 257.26       | 329.49     |
| 8    | 0.17     | 207.50       | 196.46     | 272.40       | 346.17     |
| 9    | 0.18     | 211.06       | 211.07     | 277.60       | 352.67     |
| 10   | 0.19     | 230.38       | 230.39     | 303.60       | 379.97     |
| 11   | 0.20     | 239.48       | 239.47     | 315.87       | 393.30     |

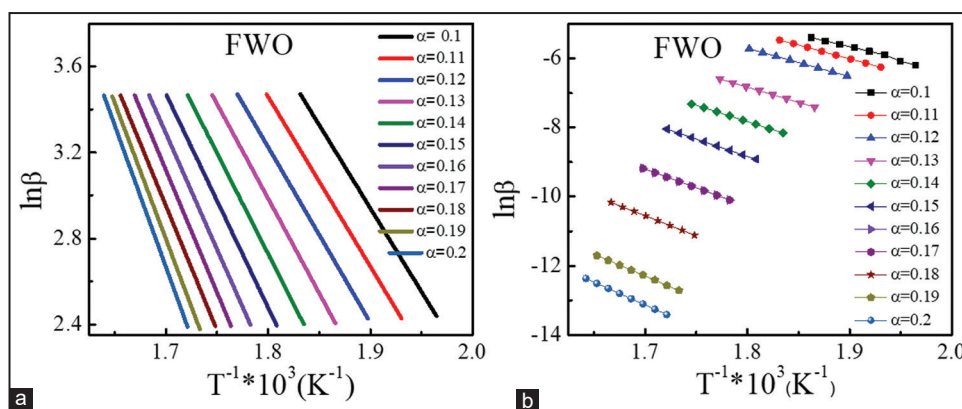


Figure 9: (a) Experimental and (b) simulation graphs of Flynn–Wall–Ozawa equation for Blocked polyisocyanate 6

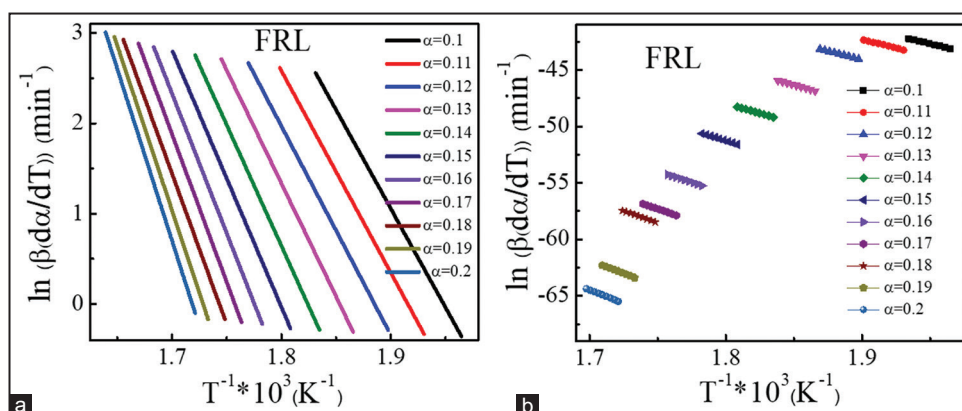
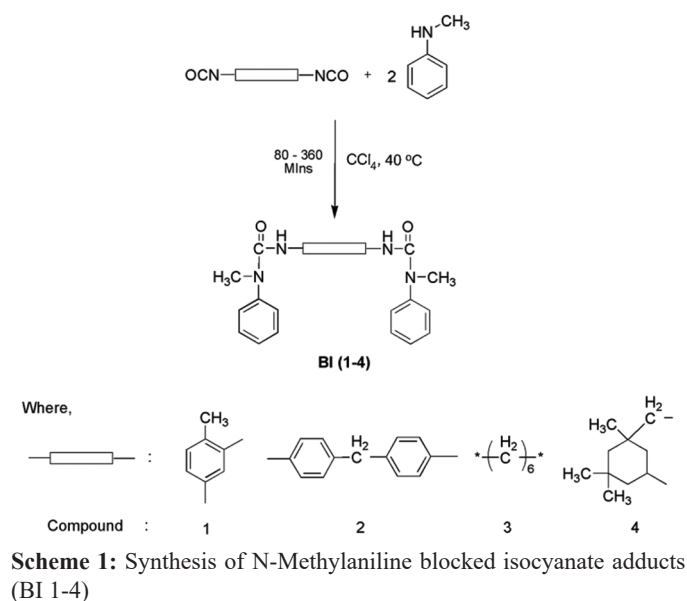
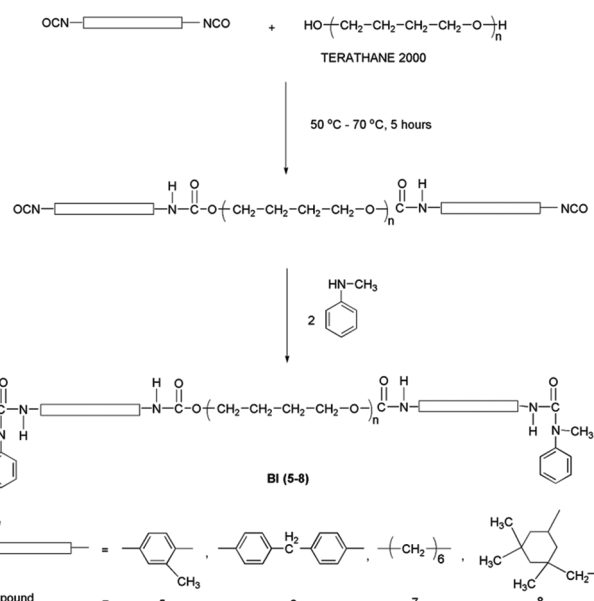


Figure 10: (a) Experimental and (b) simulation graphs of Friedmann-Reich-Levi equation for Blocked polyisocyanate 6



Ea values rise as  $\alpha$  values rise. The similar pattern may be seen in both experimental and numerical simulation data. The experimental values match the numerically calculated Ea in the FWO equation quite well. The activation energy for 0.1  $\alpha$ , which is due to the initial deblocking temperature is  $\sim 140$  and this is same for experimental and simulation for the FWO equation. As a consequence, the experimental data we got are accurate in terms of the FWO equation.



Scheme 2: Synthesis of N-Methylaniline blocked Polyisocyanates (BI 5-8)

Guo *et al.* [22] reported the slightly lesser activation energy of 134.6 kJ/mol and 126.2 kJ/mol, determined from FRL and FWO methods for pyridinol blocked IPDI. Activation energy of HDI trimer-based imidazole blocked isocyanate using the DFT method was found to be 224.7 kJ/mol [14]. Olejnik *et al.* [15] investigated heat curing PUs based on NMA blocked isocyanates and reported activation

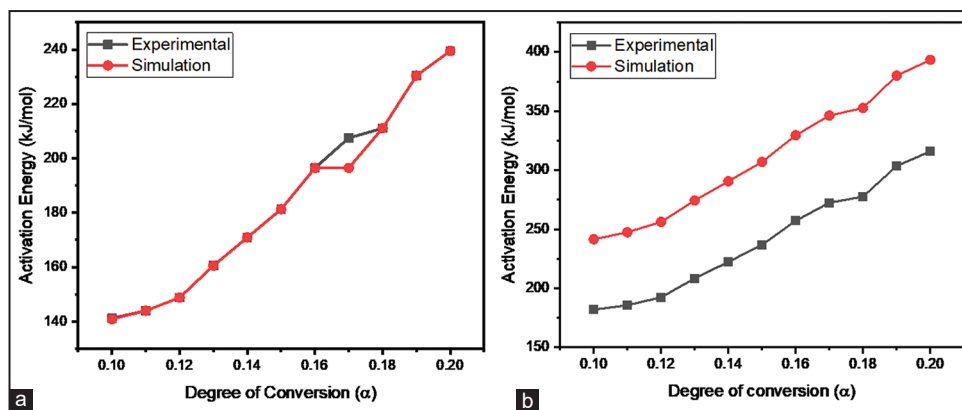


**Figure 11:** Correlation curves for degree of conversion versus activation energy using (a) Flynn–Wall–Ozawa and (b) Friedmann-Reich-Levi equation

energy as 41 kJ/mol and 47 kJ/mol using KAS and OFW methods. These results demonstrated that the activation energy highly depends on the characterization techniques, structure of the blocking agents, and isocyanates.

#### 4. CONCLUSIONS

TGA, DSC, and the CO<sub>2</sub> evolution technique were used to determine the deblocking temperatures of a series of NMA blocked diisocyanate adducts and polyisocyanates. Aromatic blocked diisocyanates deblocked at a lower temperature than aliphatic blocked diisocyanates. The deblocking temperature was discovered to be dependent on the technique and heating rate used. As the heating rate increases, so does the deblocking temperature of the blocked isocyanates. When compared to other approaches, the solution state CO<sub>2</sub> evolution approach has the lowest deblocking temperature. Ea and A for the deblocking process were calculated experimentally and theoretically using the FWO and FRL equations. The FWO equation agrees quite well with the experimental data, according to the findings of numerical simulation.

#### 5. ACKNOWLEDGMENT

The authors thank DST-SERB for financial assistance for this work. Project Sanction number ECR/2015/000172.

#### 6. REFERENCES

1. D. L. Hanks, (1991) *Bandanna-type Article of Wearing Apparel*, US Patent, No. US5058211A.
2. K. E. Martin, (2015) *Preparation of Elastic Composite Structures Useful for Components of Disposable Hygiene Products and Articles of Apparel*, US Patent, No. US9084836B2.
3. L. Mkrthyan, M. Maier, U. Huber, (2008) Structural polyurethane foam: Testing and modelling for automotive applications. *International Journal of Crashworthiness*, **13**(5), 523-532.
4. I. Panaitescu, T. Koch, V.M. Archodoulaki, (2019) Accelerated aging of a glass fiber/polyurethane composite for automotive applications. *Polymer Testing*, **74**, 245-256.
5. A. Y. Burke, N. Hasirci, (2004) Polyurethanes in biomedical applications. In: *Biomaterials*, Berlin: Springer, p83-101.
6. S. Bahrami, A. Solouk, H. Mirzadeh, A.M. Seifalian, (2019) Electroconductive polyurethane/graphenenanocomposite for biomedical applications. *Composites Part B: Engineering*, **168**: 421-431.
7. V. Stenzel, Y. Wilke, W. Hage, (2011) Drag-reducing paints for the

reduction of fuel consumption in aviation and shipping. *Progress in Organic Coatings*, **70**: 224-229.

8. J. O. Akindoyo, M. D. H. Beg, S. Ghazali, M. R. Islam, N. Jeyaratnam, A. R. Yuvaraj, (2016) Polyurethane types, synthesis and applications a review. *RSC Advance*, **6**: 114453-114482.
9. M. Fornasieria, J. W. Alvesb, E. Curti, M. Adhemar, R. Filhoc, H. Otaguroc, A. F. Rubirab, G. M. Carvalhob, (2011) Synthesis and characterization of polyurethane composites of wood waste and polyols from chemically recycled pet. *Composites Part A: Applied Science and Manufacturing*, **42**(2): 189-195.
10. A. S. Haynes, J. A. Cordes, J. Krug, (2013) Thermo-mechanical impact of polyurethane potting on gun launched electronics. *Journal of Engineering*, **42**(2): 189-195.
11. D. Turan, G. Gunes, F. S. Güner, (2016) Synthesis, characterization and O<sub>2</sub> permeability of shape memory polyurethane films for fresh produce packaging. *Packing Technology and Science*, **29**(7): 415-427.
12. D. A. Wicks, Z. W. Wicks, (1999) Blocked isocyanates III: Part A. Mechanisms and chemistry. *Progress in Organic Coatings*, **36**: 148-172.
13. D. A. Wicks, Z. W. Wicks, (2001) Blocked isocyanates III: Part B: Uses and applications of blocked isocyanates. *Progress in Organic Coatings*, **41**: 1-83.
14. M. Choi, M. G. Kim, K. I. Jung, T. H. Lee, M. Ha, W. Hyung, H. W. Jung, S. M. Noh, (2020) Reactivity and curing efficiency of isocyanate cross-linkers with imidazole-based blocking agents for low-temperature curing of automotive clearcoats. *Coatings*, **10**: 974.
15. A. Olejnik, K. Gosz, L. Piszczczyk, (2020) Kinetics of cross-linking processes of fast-curing polyurethane system. *Thermochimica Acta*, **683**: 178435.
16. C. J. Dominika, P. P. Barbara, B. Lukasz, K. Maciej, Z. Aleksandra, (2021) Hydrophobic polyurethane powder clear coatings with lower curing temperature: Study on the synthesis of new blocked polyisocyanates. *Progress in Organic Coatings*, **159**: 106-402.
17. G. Sankar, A. S. Nasar, (2007) Amine-blocked polyisocyanates. I. Synthesis of novel N-methylaniline-blocked polyisocyanates and deblocking studies using hot-stage fourier transform infrared spectroscopy. *Journal of Polymer Science Part A: Polymer Chemistry*, **45**: 1557-1570.
18. G. Sankar, A. S. Nasar. (2008) Cure-reaction kinetics of amine-blocked polyisocyanates with alcohol using hot-stage Fourier transform infrared spectroscopy. *Journal of Applied Polymer Science*, **109**: 1168-1176.

19. G. Sankar, A. S. Nasar, (2009) Effect of isocyanate structure on deblocking and cure reaction of N-methylaniline-blocked diisocyanates and polyisocyanates. *European Polymer Journal*, **45**: 911-922.
20. A. M. Issam, G. Sankar, (2011) Synthesis, deblocking and cure reaction studies of secondary alcohol-blocked isocyanates. *High Performance Polymer*, **23**(7): 535-541.
21. G. Sankar, N. Yan, (2015) Synthesis and deblocking studies of low temperature heat-curable blocked polymeric methylene diphenyldiisocyanates. *Journal of Macromolecular Science Part A: Pure and Applied Chemistry*, **52**: 47-55.
22. S. Guo, J. He, W. L. Liu, (2016) Research on the thermal decomposition reaction kinetics and mechanism of pyridinol-blocked isophorone diisocyanate. *Materials (Basel)*, **9**(2): 110.
23. Y. F. Tang, J. Liu, Z. Lil, B. Y. Chen, S. F. Mei, (2013) Study on blocking and deblocking kinetics of diisocyanate with  $\epsilon$ -caprolactam using FTIR spectroscopy. *Asian Journal of Chemistry*, **25**(10): 5703-5706.
24. Y. Zhang, J. Cao, H. Tan, J. Gu, (2014) New thermal deblocking characterisation method of aqueous blocked polyurethane. *Pigment and Resin Technology*, **43**(4): 194-200.
25. J. M. Lee, S. Subramani, Y. S. Lee, J. H. Kim. (2005) Thermal decomposition behavior of blocked diisocyanates derived from mixture of blocking agents. *Macromolecular Research*, **13**(5): 427-434.
26. M. S. Rolph, A. L. Markowska, C. N. Warriner, R. K. O'Reilly, (2016) Blocked isocyanates: from analytical and experimental considerations to non-polyurethane applications. *Polymer Chemistry*, **7**(48): 7351-7364.
27. D. W. Brazier, N. V. Schwartz, (1978) The effect of heating rate on the thermal degradation of polybutadiene. *Journal of Applied Polymer Science*, **22**: 113-124.
28. A. Ammasi, (2020) Effect of heating rate on decomposition temperature of goethite ore. *Transactions of the Indian Institute of Metals*, **73**: 93-98.
29. N. V. Kozak, K. S. Didenko, V. V. Davidenko, V. V. Klepko, (2016) Non-isothermal kinetics of  $\epsilon$ -caprolactam blocked polyisocyanate thermal dissociation. *Polymer*, **38**(4): 297-301.
30. H. L. Friedman. (1967) Kinetics and gaseous products of thermal decomposition of polymers. *Journal of Macromolecular Science Part A: Pure and Applied Chemistry*, **41**: 57-79.
31. L. Reich, W. Levi, (1968) Polymer degradation by differential thermal analysis techniques. *Journal of Polymer Science: Macromolecular Reviews*, **3**: 49-112.
32. J. H. Flynn, L. A. Wall, (1966) A quick, direct method for the determination of activation energy from thermogravimetric data. *Journal of Polymer Science Part B: Polymer Physics*, **4**: 323-328.
33. T. Ozawa, (1965) A new method of analyzing thermogravimetric data. *Bulletin of the Chemical Society of Japan*, **38**: 1881-1886.

#### \*Bibliographical Sketch



Dr. G. Sankar is an Assistant Professor at the University of Madras in Chennai, India, in the Department of Polymer Science. His research focuses on the development of novel non-conventional Blocked Isocyanates for room temperature curing systems for 1K polyurethanes, as well as the development of polymeric magnetic nanocomposites using environmentally hazardous waste and renewable resources to remove toxic effluents from industrial wastes and drug delivery applications. He has 11 peer-reviewed publications and one international patent.